CARE/JRA2: Annual Report 2007

Title: Charge production with Photo-injectors

PHIN **Coordinator: A. Ghigo (INFN-LNF)**

Deputy: R. Losito (CERN - 2007)

L. Rinolfi (CERN - 2008)

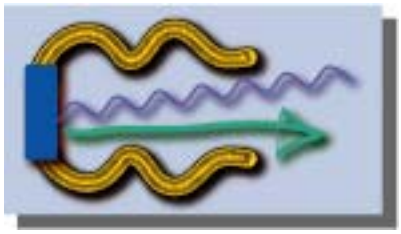

Participating Laboratories and Institutes:

Institute	Acronym	Country	Coordinator	PHIN Scientific Contact	Associated to
CCLRC Rutherford Appleton Lab. (20)	CCLRC-RAL	UK	R. Edgecock	G. Hirst	
CERN Geneva (17)	CERN	CH	G. Guignard	R.Losito	
CNRS-IN2P3 Orsay (3)	CNRS-LAL	F	A. Variola	G. Bienvenu	CNRS
CNRS Lab. Optique Appl. Palaiseau (3)	CNRS-LOA	F	A. Variola	V. Malka	CNRS
ForschungsZentrum ELBE (9)	FZR-ELBE	D	J. Teichert	J. Teichert	
INFN-Lab. Nazionali di Frascati (10)	INFN-LNF	I	S. Guiducci	A. Ghigo	INFN
INFN- Milan (10)	INFN-MI	I	C. Pagani	I. Boscolo	INFN
Twente University- Enschede (12)	TEU	NL	P. van der Slot	P. van der Slot	

Main Objectives: Perform Research and Development on charge-production by interaction of laser pulse with material within RF field and improve or extend the existing infrastructures in order to fulfil the objectives. Coordinate the efforts done at various Institutes on photo-injectors.

Cost:

Total Cost	Requested Cost
3.851 M€(FC) + 2.150 M€(AC) Total = 6.001 M€	**3.542 M€**

1. Management activities

1.1 Meeting:

CARE Annual Collaboration Meeting CERN, 29 - 31 October 2007

PHIN Collaboration Meeting Parallel session of CARE07 CERN 31 October 2007

CARE Steering Committee CERN 31 October 2007

2. Dissemination of Activity:

2.1 List of talks and conference contributions

CTF3 Collaboration meeting CERN, Geneva, January 16-17, (2007)
a) The PHIN Photoinjector for the CTF3 Drive Beam Accelerator, R. Losito
b) Laser for photoinjector, V. Fedosseev

Workshop on Laser plasma accelerators, Dusseldorf, Germany, February 12-14 (2007).
Towards a stable and tuneable compact accelerators
V. Malka (Invited)

Dream Beams Symposium, MPQ, Munich, Germany, February 25-28 (2007).
Controlled electron injection in laser plasma accelerator
V. Malka (Invited)

3rd International Conference On The Frontiers Of Plasma Physics And Technology, Bangkok, Thailand, March 5-9 (2007).
Physics and applications of laser-plasma accelerators.
V. Malka (Invited)

CLIC Meeting (CERN, 30-March 2007)
M. Petrarca "The CTF3 photo-injector laser status"

Workshop on New trends for medical applications symposium, Scotland, March 30 (2007).
Medical applications with laser plasma accelerators
V. Malka (Invited)

8th European Workshop on Beam Diagnostics and Instrumentation for Particle Accelerators - DIPAC May 20-23, Venize, Italy (2007)
Principles and diagnostics of Laser Wakefield Accelerator (LWFA)
V. Malka (Invited)

Energy Recovery Linac Workshop, Daresbury, UK, May 21 - 25 (2007)
a) J. Teichert, "Status of the Superconducting RF Photo-Injector Development"
b) F. Staufenbiel, "Beam parameter simulation of the Rossendorfer SRF gun and comparison with other RF photo injectors"

American association of physicists in medecine, Minneapolis, Minnesota US, July 22-26 (2007).
Laser plasma accelerators: high quality electron beam for radiotherapy
V. Malka (Invited)

FEL Conference, Novosibirsk, Russia, August 26 – 31, (2007)
J. Teichert, "A superconducting RF photo-injector for operation at the ELBE linear accelerator"

International Workshop on Frontiers in FEL Physics and Related Topics, Elba Island, Italy, September 8 -14, (2007)
A. Arnold, "A high-brightness SRF photo injector for FEL light sources"

Inertial Fusion Science and application, Kobe, Japan, September 9-14 (2007).
Laser plasma accelerators: towards a high quality electron beam
V. Malka (Invited plenary)

Frontiers in Optics, San Jose, California US, September 16-20 (2007).
Laser plasma accelerators: high quality and tuneable electron beam
V. Malka(Invited)

SRF Workshop, Beijing, China, October 14 – 19, (2007)
a) A. Arnold, "Reconstruction of the Field Distribution by Measuring the Fundamental Passband Frequencies of the Rossendorf SRF-Gun Cavity"
b) F. Staufenbiel, "Status of the Superconducting RF Photo-Injector Development"
c) R. Xiang, "Low emittance polarized electron source based on Superconducting RF gun"

Highlight talk of CARE annual meeting, October 29-31 (2007).
Strategies for future laser plasma accelerators
V. Malka (Invited)

CARE07 Annual Meeting, CERN, Geneva, Switzerland, October 29-31, (2007)
- J. Teichert, "The superconducting RF Gun at ELBE"

PITZ Collaboration Meeting, Zeuthen, Germany, November 26–27, (2007)
a) J. Teichert, "Commissioning of the superconducting RF gun at ELBE"
b) P.J.M. van der Slot, "Real time ellipsometry as diagnostic for Cesium-Telluride photocathodes"

2.2 List of publications

A. Barbiero, E. Chevallay, K. Elsener, R. Losito, "Caesium-Telluride Photocathode No. 166", CARE-Note-2007-018-PHIN, AB-Note-2007-023 ATB, CTF3-Note-089, https://edms.cern.ch/file/831554/7/AB_note_cathode_166_final.pdf

A. Barbiero, E. Chevallay, K. Elsener, R. Losito, "Calibration of the Thin Film Deposition Controllers in the CERN Photoemission Laboratory", AB-ATB-LPE Internal Note /EDMS No. 852732 / https://edms.cern.ch/document/852732/5

Y. Glinec, J. Faure, A. Guemnie-Tafo, V. Malka, H. Monard, J.P. Larbre, V. De Waele, J.L. Marignier, M. Mostafavi, "Broadrange single shot electron spectrometer", Care-report-06-036

V. Malka, J. Faure, Y. Glinec, A. Ben Ismaïl, A. Specka, H. Videau, "1 GeV electron spectrometer", Care report-07-034

V. Malka, J. Faure, Y. Glinec, A. Lifschitz, C. Réchatin, "Final Report on 100 MeV Laser Driven Plasma Source R&D", Care report-07-031

V. Malka, A. Lifschitz , J. Faure, Y. Glinec, "GeV monoenergetic electron beam with laser plasma accelerator", International journal of modern physics B 21, (3-4), p277-286 (2007).

J. Faure, C. Rechatin, A. Norlin, F. Burgy, A. Tafzi, J. P. Rousseau, V. Malka, "Controlled injection in laser plasma accelerator", Plasma Physics and Controlled Fusion 49 B395-B402 (2007).

A. Arnold, H. Büttig, D. Janssen, U. Lehnert, P. Michel, K. Möller, P. Murcek, Ch. Schneider, R. Schurig, F. Staufenbiel, J. Teichert, and R. Xiang, T. Kamps, D. Lipka F. Marhauser, W.-D. Lehmann, J. Stephan, V. Volkov, I. Will, G. Klemz "Development of a superconducting radio frequency photo injector" Nucl. Instr.and Meth. A577 (2007) 440

S. Cialdi, C. Vicario, M. Petrarca and P. Musumeci, "Simple scheme for ultraviolet time-pulse shaping" Applied Optics 46 (2007) 4959.

M. Boscolo, M. Ferrario, C. Vaccarezza, I. Boscolo, S. Cialdi, F. Castelli, "A train of micro-bunches for PWFA experiments produced by RF-photoinjectors", Int. J. Mod. Phys. B 21, (2007) 415.

M. Boscolo, M. Ferrario, I. Boscolo, F. Castelli and S. Cialdi, "Generation of short THz bunch trains in RF-photoinjectors" Nucl. Instr. and Meth. A 577 p.409-416 (2007).

M. Boscolo, M. Ferrario, I. Boscolo, F. Castelli and S. Cialdi and V. Petrillo' "Generation of a multipulse comb beam and a relative twin pulse fel" in PAC Proceedings, Albuquerque, NM, 2007

M. Boscolo, I. Boscolo, F. Castelli, S. Cialdi, M. Ferrario, V. Petrillo, C. Vaccarezza, "Generation of comb electron beams and of neat FEL radiation spikes" presented at the Elba-Italy October 2007 FEL workshop and to be published in NIM Phys. Res. A

M. Boscolo, I. Boscolo, F. Castelli, S. Cialdi, M. Ferrario, V. Petrillo, C. Vaccarezza, "Single spike operation in SPARC SASE-FE" presented at the Elba-Italy October 2007 FEL workshop and to be published in NIM Phys. Res. A

S. Cialdi, C. Vicario, M. Petrarca, P. Musumeci, Appl. Opt. 46, 22 (2007) 4959-4962.

C. Vicario, et al, Proceedings of PAC07 TUPMN040, Albuquerque, New Mexico, USA

C. Vicario et al. SPARC Technical Note LS-07/001, 23/05/2007 http://www.lnf.infn.it/

C. Vicario et al. SPARC Technical Note LS-07/002, 23/05/2007 http://www.lnf.infn.it/

M. Tesselaar. “Real-time Ellipsometry on Cesion-Telluride Photocathode Formation and Multiphoton Photoelectric Emission frrom Copper”. Master Thesis, University of Twente.

WP 2, CHARGE PRODUCTION

CERN

Production of photocathodes has been re-started after more than 4 years. A Quantum Efficiency (QE) of 6.2 % has been measured on a new photocathode (number 166), produced in the preparation chamber of the photocathode laboratory. An image of the electron beam observed on a scintillating screen is shown in Figure 1. This result, measured using the DC gun in the photoemission laboratory, is very encouraging taking into account the fact that a QE of 3% is specified for CTF3 operation and that the preparation chamber could not be baked out due to several minor mechanical problems that have been solved during 2007. The full bake out of the preparation chamber is progressing and baseline production of photocathodes for the photoinjector commissioning has started in December 2007.

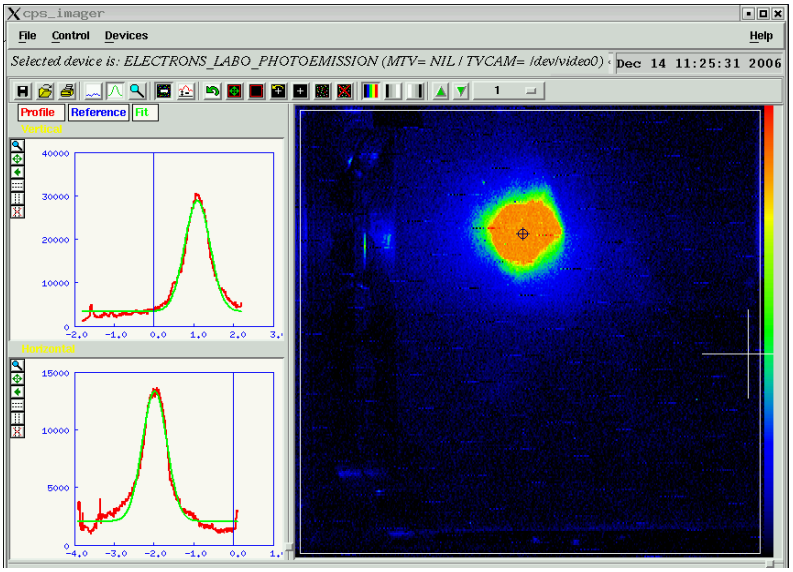

Figure 1: Image of the electron beam produced in the photocathode laboratory. The Cs-Te photocathode 166 is illuminated with UV laser light, and the photoelectrons produced are accelerated in the 80 kV DC gun.

A collaboration agreement established with the University of Naples "Federico II" provided the basis for presence at CERN at full time for one year of a young researcher, Andrea Barbiero, who designed a new Ultra High Vacuum (UHV) transfer arm. The goal of this new arm is to provide a lighter structure to transport photocathodes produced in the photocathode laboratory to the XPS laboratory of the CERN-TS/MME group, allowing a deeper investigation of the relationship between deposition parameters and compounds of Cesium and Tellurium present in the thin film deposed on the photocathode. Study of the effect of contamination on QE and on photocathode lifetime is also envisaged. The mechanical design (see for example Figures 2 and 3) has been completed and approved, and procurement of the different components is in progress.

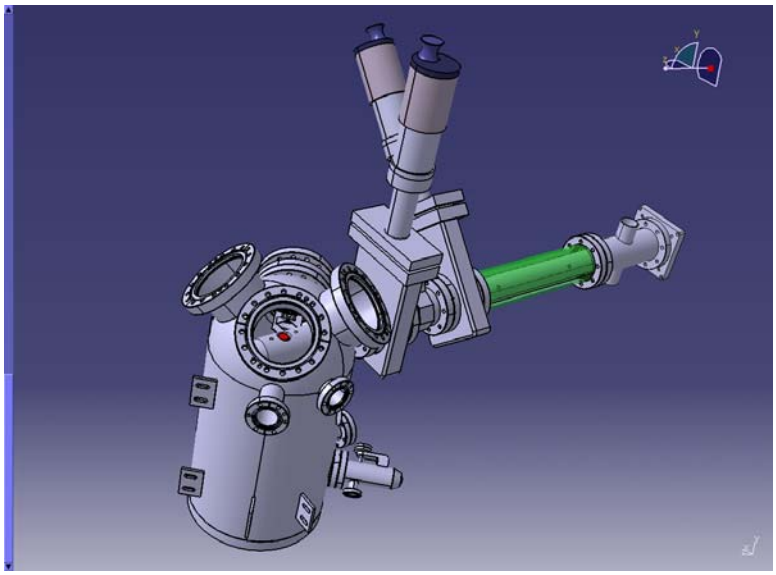

Figure 2: CATIA design image of the new transfer arm (in green the manipulator) connected to the XPS chamber.

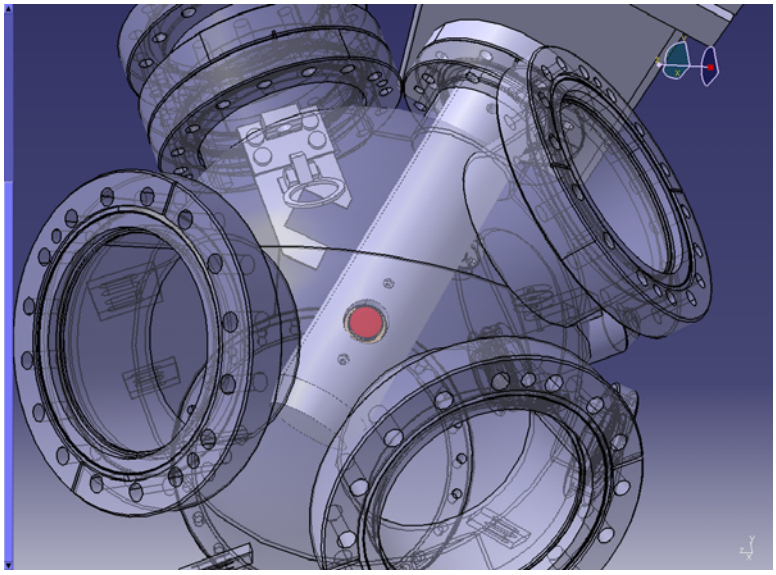

Figure 3: CATIA design image of the photocathode (in red) in position for XPS measurements.

A Stylus profiler (Figure 4) has been purchased and installed in the laboratory to measure the thickness of the coatings, to obtain a precise calibration of the thickness deposited during the process. This is particularly important to ensure a repeatable stoichiometric ratio of the Cs-Te film. The performance of this instrument is regularly checked using a Taylor-Hobson calibrated sample. A typical calibration measurement is shown in Figure 5.

Figure 4: The new Dektak 6000 Stylus Profilometer (left). Measurement of a quartz test sample with a Te coating (right). Standard film thicknesses are of the order of 20-50 nm.

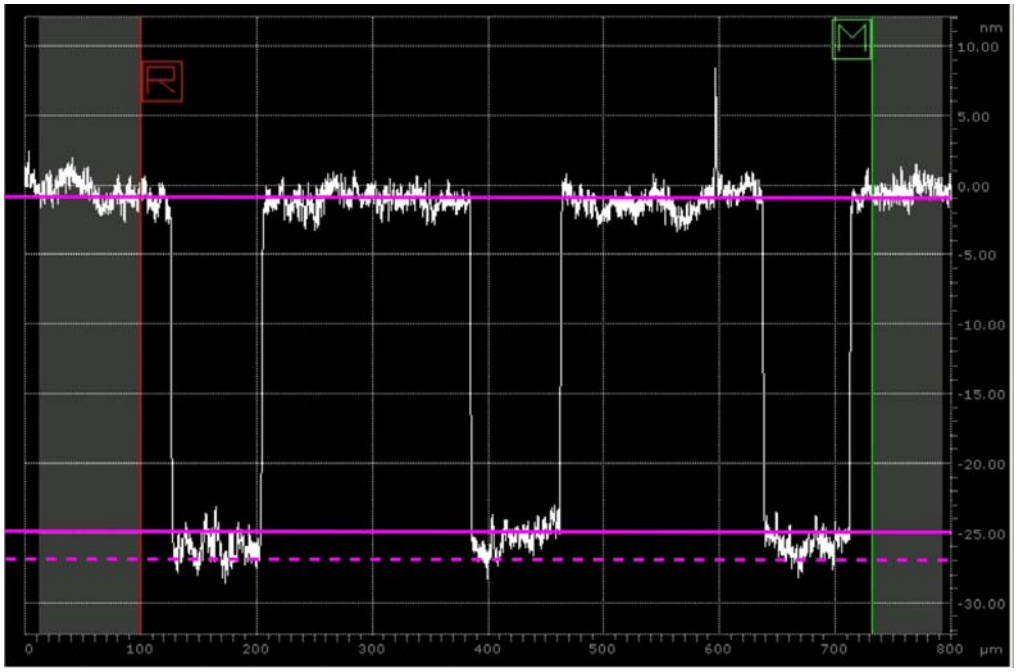

Figure 5: Measurement of a calibrated Taylor-Hobson sample with three 24 nm deep groves. Solid lines in the image are 24 nm apart; the dashed line indicates an additional 2 nm. Conclusion: The accuracy of the Stylus Profilometer is better than 2 nm.

LAL

The vacuum tank designed to make alkaline deposits on photocathode substrate has been machined in the LAL workshop. In addition the vacuum transfer system and the large ionic pump which have been ordered to private companies are available at LAL. But a leakage problem due to the large aluminum gasket is under investigation.

LOA

Plasma-based accelerators have been proposed for the next generation of compact accelerators because of the huge electric fields they can support. However, it has been difficult to use them efficiently for applications because they produce poor quality particle beams with large energy spreads. By focusing light pulses containing a few joules of energy in a few tens of femtoseconds onto gas jets, extremely large electric fields can be generated, reaching the teravolts per metre level. As a result, the length over which electrons extracted from the target can be accelerated to hundreds of MeV is reduced to a few millimetres. The reduction of the size and the cost of laser plasma accelerators is a promising consequence, but these electron beams also reveal original properties, which make them a wonderful tool for science. By adjusting the interaction parameters, the electron energy distribution can be tuned from a maxwellian-like distribution to a quasi monoenergetic one. The new properties of these laser-based particle beams are well suited to many applications in different fields, including medicine (radiotherapy), chemistry (ultrafast radiolysis), material science (non-destructive material inspection using radiography) and, of course, for accelerator physics. The purpose of our contribution in the project was the development of compact single shot electron spectrometers in order to optimise the coupling of the laser beam into the electron beam and especially to control the electron distribution energy. This has allow us to understand specific feature of the interaction, to demonstrated new scheme of injection (bubble and colliding), and to explore new applications. A complete document which reports the LOA/CARE activities on this field can be found on the CARE website as CARE report 07-031. Figure 6 presents the major result obtained this year using two counter propagative laser beam.

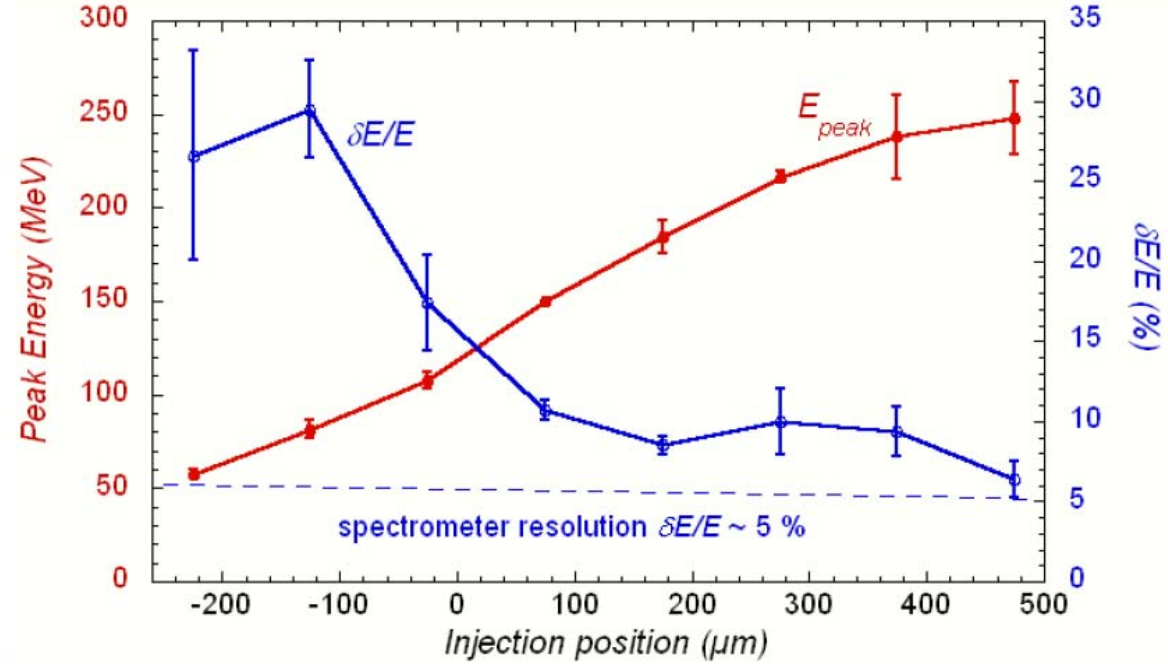

Figure 6: Evolution of the electron beam peak energy (red curve and left vertical axis) and its energy spread (blue curve and right vertical axis) versus the injection position z_{inj}, e.g. the position at which the two laser pulses collide. Each point is an average of 3-5 shots and the error bars correspond to the standard deviation. The position z_{inj}=0 corresponds to injection at the middle of the gas jet, whereas z_{inj}=500 μm corresponds to early injection close to the entrance of the gas jet.

FZR

The construction of the photo cathode preparation system at the FZD and the development of the preparation technology for cesium telluride photo cathodes were finished. In 2007, the preparation system was equipped with an Ar sputter ion gun of the company SPECS. The ion gun is used for pre-cleaning of new photo cathodes and rejuvenating used photo cathodes. In order to improve the vacuum, heating jackets for the exchange and storage chambers were bought. In detail the preparation system has the following features now:

1.exchange and storage system for six photo cathodes,
2. photo cathode heating,
3. evaporator for Cs and Te with heating power control,
4. precision positioning system for the evaporators,
5. deposition rate monitors,
6. cathode shutter,
7. anode grid with high voltage for photo current measurements,
8. UV laser system for Q.E. measurements and cathode scanning,
9. ion sputter gun for cathode cleaning,
10. vacuum system with ion getter pumps and residual gas mass spectrometer,
11. hard- and software (Visual C++) for computer controlled deposition.

The main part of the man power was used for the development and optimization of the preparation technology. Especially the design of the evaporators was improved. For tests a number of photo cathodes have been prepared and measured using the standard procedure (Te and Cs in succession) as well as the co-evaporation process. As an example the Figures 7 and 8 show the results of the Q.E. measurements of a cathode produced by co-evaporation with a Q.E. of about 7 - 8 % after deposition. The SRF photo gun at FZD requires a Q.E. > 1 %.

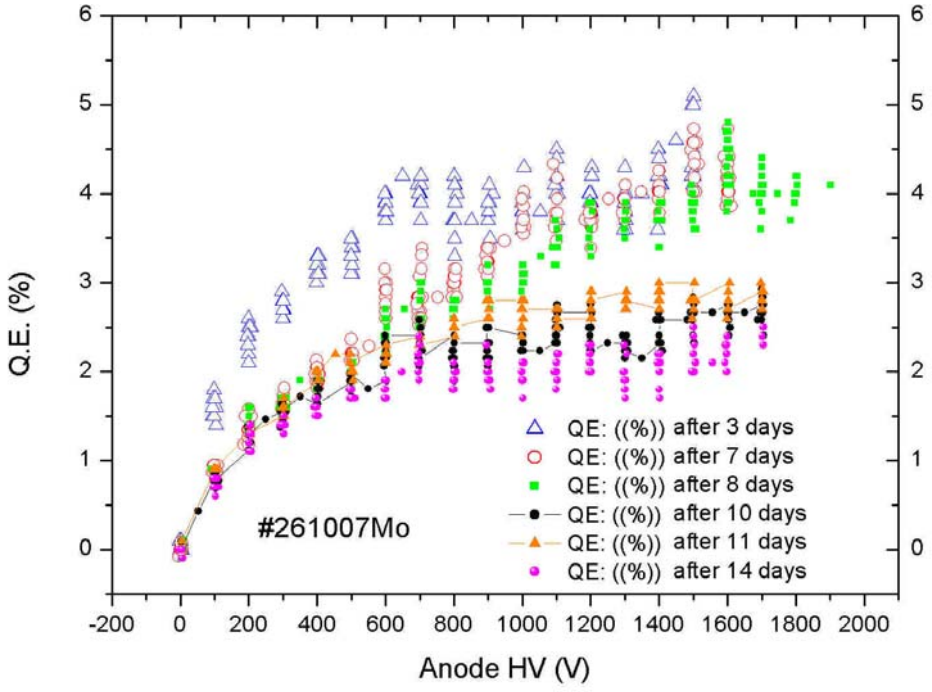

Figure 7: Measurement of the quantum efficiency of a Cs_2Te photo cathode produced by co-evaporation after different storage time.

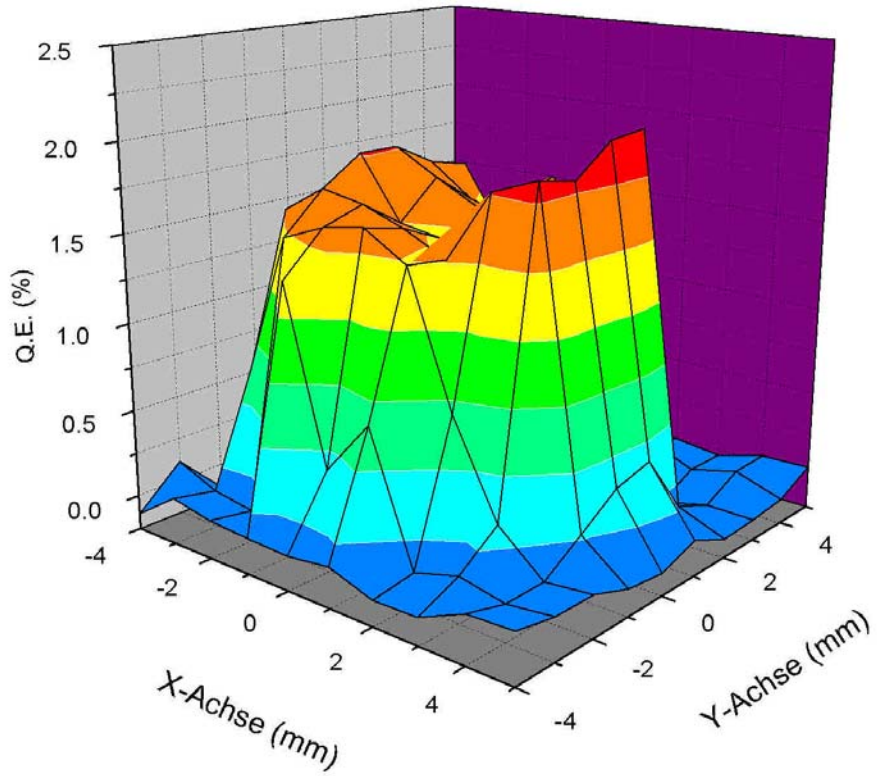

Figure 8: Q.E. distribution measured for the photo cathode #261007.

The second photo cathode transfer system was assembled and tested. It will be installed at the superconducting RF photo gun in the winter shutdown of ELBE in January/February 2008. After installation of the system, Cs_2Te photo cathodes can be moved from the preparation system to the SRF gun, inserted and used in the gun without breaking the vacuum. The present studies and measurements at the SRF gun are carried out with a Cu photo cathode.

At FZD, the work in work-package 2 of PHIN had been carried out by a postdoc (Dr. Rong Xiang) until November 2007 paid by the CARE project. After a break (maternity leave) the work will be continued in 2008 with payment from FZD.

TEU

During the reporting period, Dr J. Verschuur has left the group and Dr van der Slot has taken over his tasks. TEU has focused on implementing diagnostics for photocathode research and mainly on using ellipsometry for studying the formation of the layers during the growth of the photocathode. For that reason, we have implemented an interferometric ellipsometer and found that the cathode vibrations were too large to successfully use this type of ellipsometer. We therefore changed the ellipisometer into a rotating compensator ellipsometer (see Fig. 9).

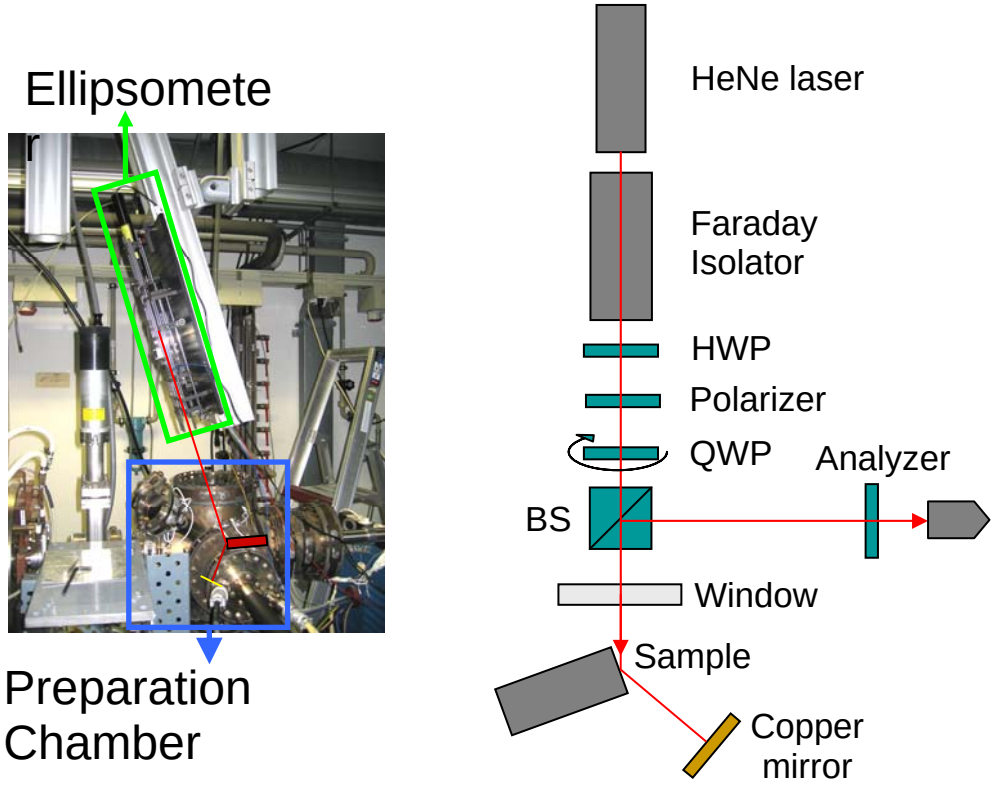

Figure 9. Rotating compensator ellipsometer

This elllipsometer was successfully used to measure the reflected signal of the photocathode during the deposition of Te and Cs. An example of the data retrieved from the reflected signal is shown in Figure10.

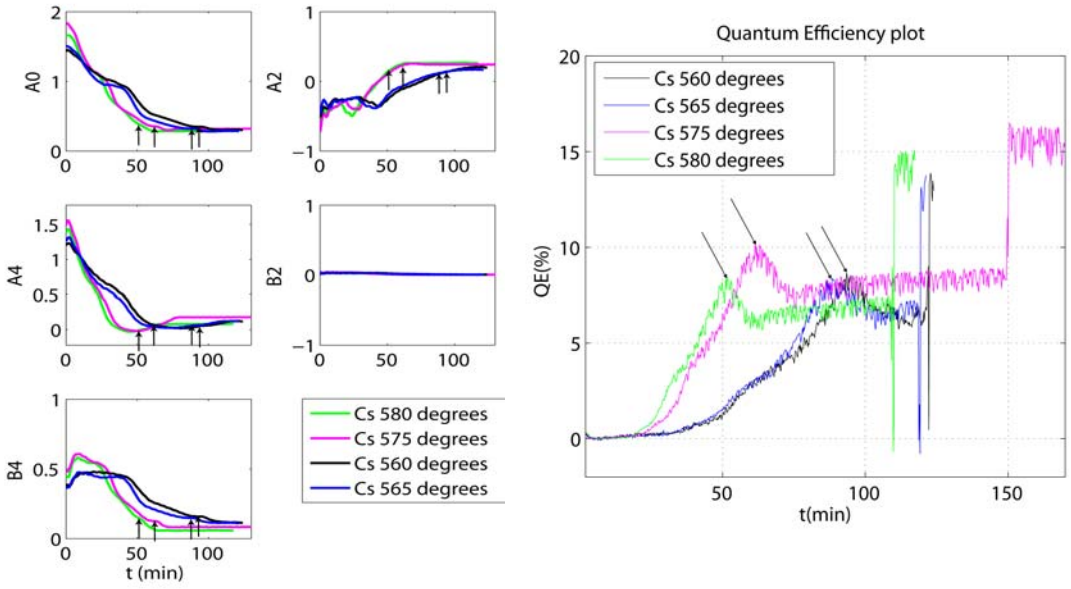

Figure. 10. Ellipsometric coefficients A0 to B4 and quantum efficiency plot for various deposition temperatures of Cs.

These measurements show that different traces are recorded for different deposition temperatures of Cs during the growth of the photocathode. This seems to indicate that layers are formed with different properties during the formation of the photocathode, depending on the exact deposition rate of the Cs. We were not able to retrieve the ellipsometric variables from the measured data, and therefore the physical parameters of the layers, because we have insufficiently characterized the complete setup. Work to do this is currently underway and further improvements on the elllipsometer are being implemented. So far, the rotating compensator ellipsometer seems able to supply additional in-line information on the formation of the photocathode during production, and may therefore be a very interesting diagnostic tool for growing photocathodes.

WP3, LASER

RAL

No work has been carried out at RAL for PHIN in 2007.

CERN

The design of the laser has been performed by Rutherford Appleton Laboratory but its construction was not completed before the shipment to CERN in 2006. A considerable delay has therefore been accumulated on the laser milestones since CERN had not foreseen in the project manpower for laser construction, but only for operation. To compensate the lack of manpower and competence, an associate from RAL was hired for six months in 2006 to help with construction and commissioning, but the contract was stopped after three months. Several severe hardware failures have delayed even more the project, since the laser oscillator and amplifier were not available for several months.
Informal collaborations were therefore established with INFN Frascati and INFN Milano, partners of PHIN but not previously involved in the photoinjector for CTF3, to fill the gap.
INFN Milano accepted to take responsibility for demonstrating the feasibility of the phase coding scheme proposed by RAL which makes use of custom "Off The Shelf" components for telecommunications.
INFN Frascati, that is developing a photoinjector for SPARC, has experienced laser scientists, and accepted to send them to CERN to help commissioning the amplifier chain.

By the end of 2006 the laser was partially assembled and the oscillator, the preamplifier and the first amplifier had been commissioned. Commissioning of the second amplifier was started in 2007. The output power of the first amplifier is satisfactory (see Figure 11) and in agreement with the specifications. The second amplifier was found below the specified value of 15 kW (see Figure 12).

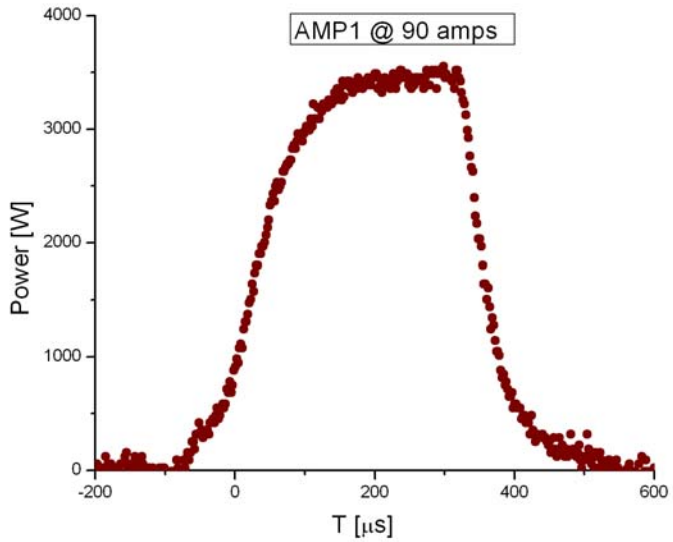

Figure 11. The power-time plot of the laser pulse train at the output of the first amplifier. The time window during which the amplification takes place is of 400 μs.

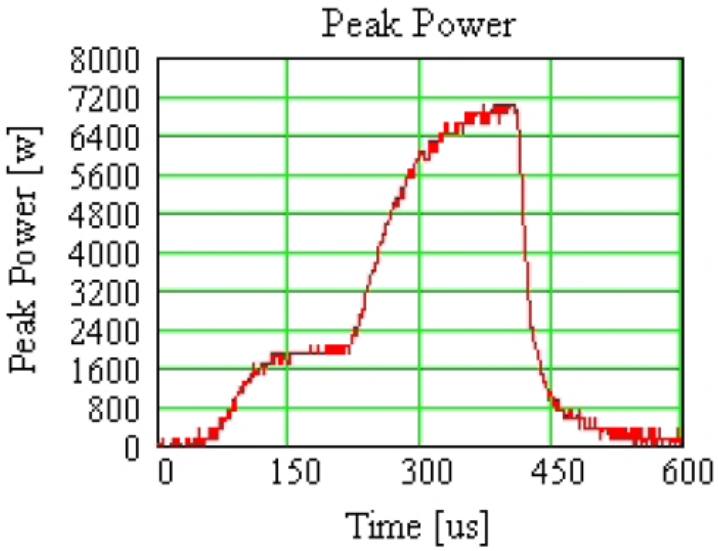

Figure 12. The power-time plot of the laser pulse train at the output of the second amplifier. The time window during which the amplification of the second amplifier takes place is of 200 μs and starts with a delay of 200 μs after the beginning of the first amplifier amplification.

The study of factors defining the amplification of laser power was carried out with participation of the scientific associate M. Petrarca from INFN Frascati, who will be more involved on the laser improvement, maintenance and installation from 1st January 2008 under a fellow contract at CERN. It was found that the beam size should be carefully adjusted for optimal matching to the Nd:YLF rod aperture of the second amplifier and to maintain the beam collimated during the propagation of beam into the amplifier while this is working at full power. To that purpose a three lens system was installed; with this optical system it is possible to introduce a magnification of the beam size while keeping the rays almost collimated. The layout of the laser is shown in Figure 13.
It has also been found that the optical pumping power of the second amplifier is below the specification, i.e. ~15KW compared to ~25 KW. To understand the reason for this fact, communication with the RAL people involved in the laser amplifier project is foreseen in 2008.

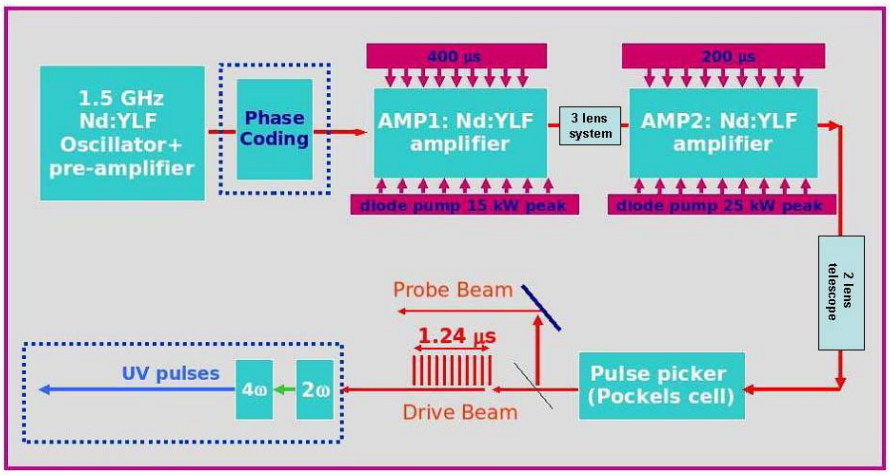

Figure 13: Layout of the laser setup for the CTF3 photoinjector.

It should be mentioned that the same laser will supply laser pulse bunches for the CTF3 probe beam photoinjector. This project is called CALIFES (Concept d'Accélérateurs Linéaire pour Faisceau Sonde). To that purpose the laser pulses remaining after the bunch slicing with the Pockels cell are to be directed to the CALIFES pulse picker and frequency multiplication system. Setting up of the CALIFES laser beam was started in 2007 in collaboration with CEA Saclay.
A two lenses system has been installed between the second amplifier and the Pockels cell in order to match the fully amplified beam size with the Pockels cell crystal dimension.

The shape and divergence of the laser beam produced are important parameters for efficient generation of the required UV 262 nm beam by means of frequency multiplication in non-linear crystals. The measurements of the oscillator and preamplifier laser beam quality were performed using the beam propagation analyzer Spiricon M2-200. An example of such measurement is presented in Figure 14.

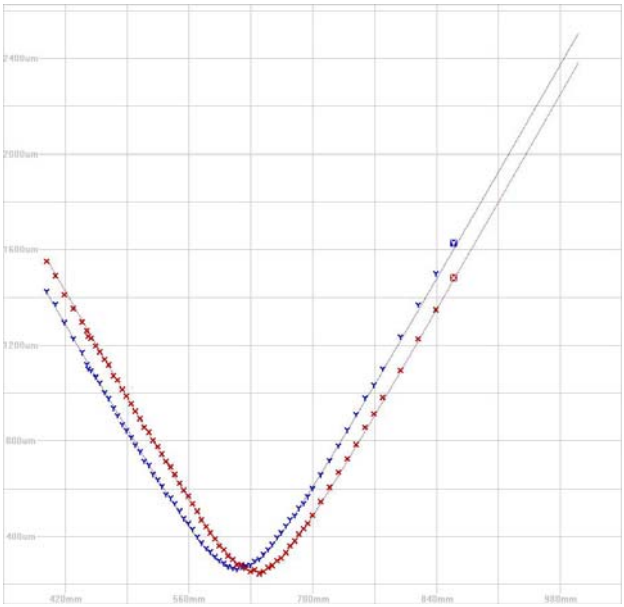

Figure 14: Snapshot of the measurement of laser beam divergence after the preamplifier, using the beam propagation analyzer Spiricon M2-200; on the vertical axis the beam width is reported in micron (200 μm per division), on the horizontal axis the beam propagation distance in millimetre from the input face of the Spiricon device (70 mm per division) is reported. The measured divergence parameters M^2 are: 1.23 for the X-plane and 1.27 for the Y-plane.

Measurements regarding the M^2 values for the full amplified beam gave a result between 2 and 2.8. Therefore, further studies on the possibility to improve the beam quality during amplification were made, resulting (Jan. 2008) in a value of ~1.8 for the M^2 along the X- and Y-plane. These measurements have been performed by M. Petrarca (CERN) and G. Cheymol (Saclay). Even though better results have been obtained showing a better quality of the transverse beam shape, further studies are foreseen to improve it even more.

Unfortunately, the work has been hampered by numerous hardware faults. In particular, two drivers for the amplifier pumping diode laser stacks were sent one after another to the manufacturer (Laselec) for repair (inside the warranty period). During a long period the commercial laser preamplifier (High Q Laser) was not operational because of a construction

error, admitted by its manufacturer. Some problems in the laser cooling system also had to be identified and solved.
The major problem remaining in the amplification chain is the lack of power, in fact 15 KW of peak power were foreseen in the design from the RAL laboratory but only ~9.5 KW are now available.
The reason for this is to be imputed to the second amplifier which is under further studies. The 15KW of pumping power actually available to drive the second amplifier compared to the 25KW originally foreseen in the RAL design could be one of the main reasons.

The R&D work on laser pulse phase coding was carried out in collaboration with INFN Milano. The components of the phase coding system were sent to Milano. In a result of tests which have been carried out there, the feasibility of the approach based on fiber optics was demonstrated, although substantial losses of laser power at the beam injection into single-mode fibers are to be taken into account (see below INFN-MI).

INFN – LNF

The shaping of ultrafast laser pulses is of increasing interest in a wide variety of optical applications, including quantum and optimal control, high speed communications and material characterization. The promise of increasing the brightness of electron beams from RF (radio frequency) photoinjectors by using a flat top UV laser pulse to illuminate the cathode is the application inspiring the work presented here. For optimum driving a photocathode of a S-band RF cavity, such as the SPARC photoinjector, one desires ideally a relatively high energy (> 100μJ) UV laser pulse 5 to 10 picoseconds long, with a flat top temporal profile having fast (~ 1ps) rise and fall times. The current techniques to manipulate the bell shape laser pulse employ devices that work in the IR, in general before the amplification. This set up requires the pulse shapers are able to compensate the unavoidable distortions caused by the amplification and the harmonic. To perform this pre-compensation is in general advisable to work with programmable shapers. We review here two most widespread techniques: one is based on a programmable dispersive acousto-optic modulator (the DAZZLER) while the other is based on a liquid crystal mask spatial light modulator (LCM-SLM) placed in a 4-f optical setup.
The described techniques are well-known but, according to our knowledge, the two pulse shapers have never been directly compared in the same experimental conditions. We present the performances of the two devices tested with the SPARC laser system in the frame of CARE collaboration.

The principle of laser pulse shaping in time domain is based on the amplitude and phase modulation of the spectral components. The field of a light pulse has, in the time and frequency domains, respectively, the expressions:

$$E(t) = \sqrt{I(t)}\, e^{i\Phi(t)} e^{-i\omega_0 t} \qquad \widetilde{E}(\omega) = \sqrt{\widetilde{I}(\omega-\omega_0)}\, e^{i\widetilde{\Phi}(\omega-\omega_0)} \qquad (1)$$

The pulse shaping manipulation is a linear filtering process. In the time domain the filter action of the shaper is represented by an impulsive response function h(t); in the spectral domain the filter action is represented by the Fourier transform H(ω) of h(t). The output electric field $E_{out}(t)$ is the convolution of the input $E_{in}(t)$ and the response function h(t): $E_{out}(t) = h(t) \otimes E_{in}(t)$. In the frequency domain we can write: $\widetilde{E}_{out}(\omega) = H(\omega) \cdot E_{in}(\omega)$.

In general H(ω) is a complex function that can be decomposed as an amplitude and phase terms: $H(\omega)=T(\omega)e^{i\phi(\omega)}$. Appropriate T(ω) and phase ϕ(ω) modulation can lead to any kind of output signal compatible with the original spectral width. When the input and output fields are given and it is possible to introduce both amplitude and phase modulation the solution of the problem is unique. This solution can be computed by using those particular functions T(ω) and ϕ(ω) that make the Fourier transform of the input equal into the Fourier-transformed output. Nevertheless, in order to obtain the target pulse, it is possible to apply only an appropriate phase function modulation; in this case there are multiple solutions to the problem of find the filter transfer function.

EXPERIMENTAL SETUP FOR SPARC LASER

The experimental set-up used to perform the comparison between the two pulse shapers is reported in Figure 15. Due to their low optical damage threshold and relatively high insertion losses, the two devices are placed immediately after the Ti:Sa oscillator (central wavelength 800 nm, repetition rate 79.3 MHz and ~6nJ energy per pulse).

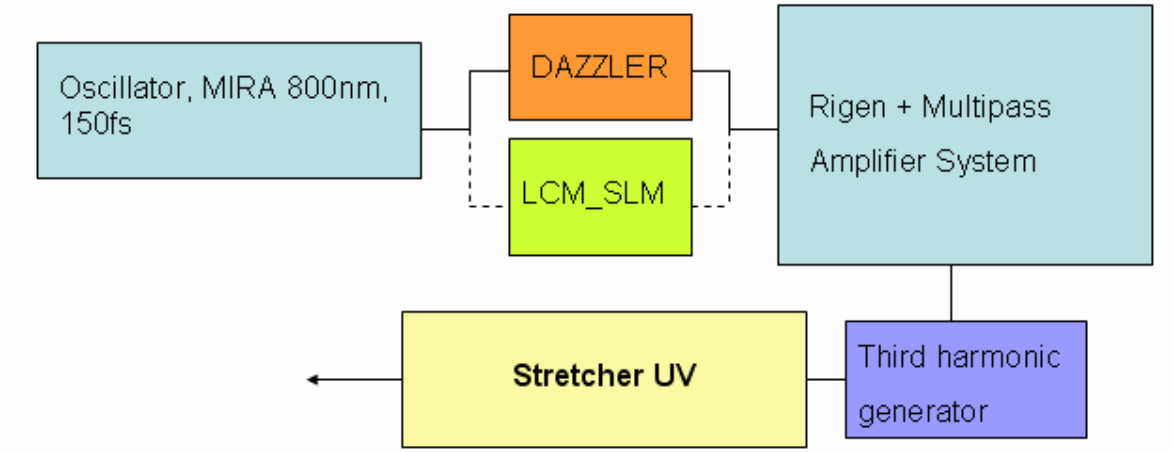

Figure 15: SPARC laser system; the two pulse shapers are easily interchangeable.

The amplification process is carried out by one regenerative pre-amplifier and a two double passes stages. The system delivers 100 fs pulses with energy of about 50 mJ and a repetition rate of 10 Hz.
At the output of the amplifier the IR pulses go to a third harmonic generator, where UV pulses with energy of up to 4 mJ are produced. At the end of the laser chain there is a stretcher based on a pair of 4350 groove/mm UV reflecting gratings that is used to stretch temporally the pulses up to 15 ps. The utility of a UV stretcher placed after the harmonic generation is motivated by two principal reasons:

1) The stretcher is necessary in order to maximize the third harmonic conversion efficiency obtaining the maximum UV energy on the cathode; in fact it allows us to temporally lengthen the UV pulses width after the harmonic conversion process whose efficiency depends on the input optical peak power.

2) The UV stretcher introduces a tight binding between the UV spectral and time profile of the laser pulses. In fact, the spectral profile is transferred into the time profile due to the large linear chirp introduced by the stretcher. This consideration, obviously,

simplifies the search of the optimal spectral phase and amplitude modulation. Moreover the direct correspondence time-spectral shape makes straightforward the reconstruction of the pulse time intensity using a single shot high resolution diagnostic.

To find the optimal pulse shaper's phase and amplitude modulation to apply we developed the ORFEO code in Labview environment (see Figure 16). This software tool calculates the second and third harmonic time profile and spectra starting from the measured fundamental harmonic spectral intensity. It is possible to apply an arbitrary spectral phase function and observe the changes on the harmonics time and wavelength intensities. The program includes also the distortions of possible non-linear crystals angular mis-alignment. Finally it is possible to simulate the linear chirp added with the UV stretcher.
The ORFEO code demonstrated to be useful and reliable tool and, it allows the direct comparison with the experimental data we presented in previous papers. In the figure 2, the ORFEO screenshot is reported: the upper row from left to right shows the experimental IR spectrum, the second and third harmonic wavelength domain intensity. The lower row reports the corresponding calculated IR, blue and final UV time intensity. At the bottom, some knobs are noticeable; these visual inputs permit to synthesize the proper spectral phase function. The UV stretcher's chirp and the non-linear crystal angle deviation from the phase matching condition can also be simulated.

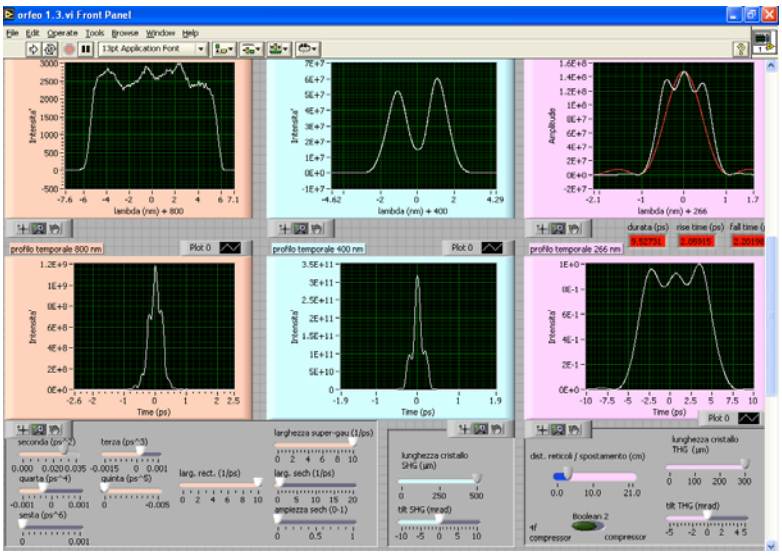

Figure 16: ORFEO code screen shot.

DAZZLER PULSE SHAPER

The "DAZZLER", an "Acousto Optic Programmable Dispersive Filter", is a system designed by FASTLITE to manipulate the spectral phase and amplitude of ultrafast laser pulses.
A RF signal within 40−50 MHz excites a piezo transducer which generates an acoustic wave inside an bi-refrangent acousto-optic TeO_2 crystal. The acoustic wave propagates along the crystal spatially reproducing the RF signal. Being the optical wave velocity much greater than the acoustic wave velocity, the input optical pulse propagates as trough a fixed dielectric grating inside the crystal. The two linear optical modes of the crystal can be efficiently coupled by an acousto-optic interaction when the phase matching condition, energy and

momentum conservation, between the acoustic wave and the two optical modes are satisfied. The coupling condition assures a partial energy transfer from the input to the output optical mode. The two modes emerge out of the crystal at different angle and the part of the optical pulse interacted with the acoustic grating can be easily separated from the un-diffracted one, and then it can be amplified. The efficiency of the interaction for an optical wavelength depends on the amplitude of the corresponding acoustic frequency. Therefore by controlling the amplitude of the acoustic spectrum it is then possible to perform an amplitude modulation of the optical frequencies.

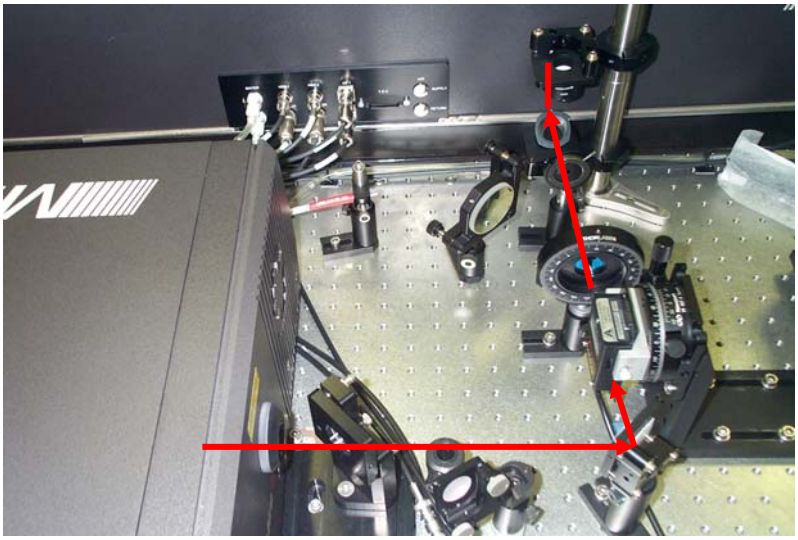

Figure 17: Dazzler set-up: the oscillator output is sent to the acousto-optic filter and a half wavelength wave-plate. After, a periscope is used to inject the beam in the amplifier.

Sending RF chirped signal in different position z along the crystal there will correspond different acoustic frequencies. Since locally, for a given z, there is just one spatial frequency in the acoustic grating, only the optical frequency that satisfy the phase matching condition, can be diffracted in that position z. In this way it is possible to diffract different frequencies at different depths. Due to the TeO_2 birefringence two wavelengths experience diverse propagation time and are subjected to different phase modulation.
The Dazzler we used is composed by a 2.5 cm acoustic material. It has a resolution of 0.3 nm and work over a bandwidth of 200 nm around 800 nm. The maximum chirp can apply produce a laser pulse up to 6 ps. The energy losses reach about 50 %.
As shown in the Fig. 17 the DAZZLER is mounted at the oscillator's exit and because polarization of the laser pulse is rotated by the acousto optic interaction, we use a lambda/2 waveplate prior to send the beam into the amplifier.
Our procedure to seek the flat top pulse is based on the search of the proper phase and amplitude modulation to obtain the target third harmonic spectrum profile that corresponds to the wanted time profile. As said before the target temporal pulse is obtained by generating a UV rectangular spectrum and then converting it into a rectangular temporal shape by the stretcher. To have the flat top spectrum at 266 nm we start generating a square-like spectrum after the DAZZLER and with proper amplitude modulation, pre-compensate the distortion introduced by the amplifier. In this way it is possible to have a flat top pulse out of the Hidra compressor.
As said before, it is not possible to produce directly 10 ps rectangular IR pulse before the harmonic generation because otherwise the conversion efficiency of the two BBO crystals would result too low. At the same time it is important to stress that it is not possible for the IR laser pulses to enter the crystals with temporal pulses that are too short. In fact, the generated

second harmonic and third harmonic spectral widths depend strongly on the first-harmonic pulse length.

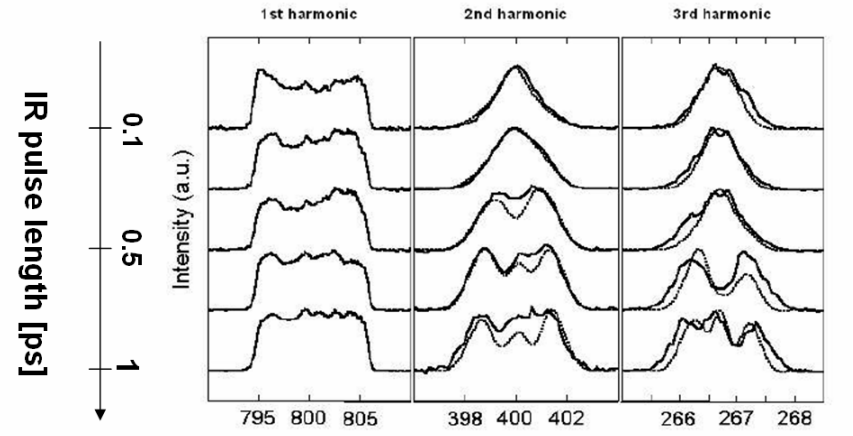

Figure 18: From left to right: measured (solid curve) and simulated with ORFEO (dashed curve) IR, BLUE, and UV spectra. Starting from a transform-limited pulse.

This behavior is shown in Figure 18 by reporting the changes that occur in the spectrum of the second harmonic and third harmonic signals as a function of the chirp introduced by the DAZZLER. In the left part of the figure the first-harmonic spectra shaped by the DAZZLER are presented; the middle and the right parts show the experimental and calculated second harmonic and third harmonic spectra, respectively. Starting from a transform-limited pulse, we increase the chirp by 0.01 ps^2 for each curve from top to the bottom. As shown in the figure there are a good agreement between the measured spectra and the ones simulated by ORFEO. The DAZZLER phase function was set to have a IR pulse enough long, 0.7 ps, to preserve the flat spectrum trough the non linear crystals, and at the same time keep the third harmonic efficiency high. Using the amplitude modulation to have a flat top amplified IR spectrum and a proper phase modulation to keep the flat top spectral shape trough the third harmonic generator it was possible to have a reasonable square-like UV pulse in time. In the Figure 19 is reported the UV pulse obtained with the DAZZLER shaper we measured with the multi-shot cross-correlator. The rise time obtained is about 2.6 ps and the oscillation on the plateau is limited to the 30 % ptp. The oscillation takes into account also the shot-to-shot instability of 5 % rms

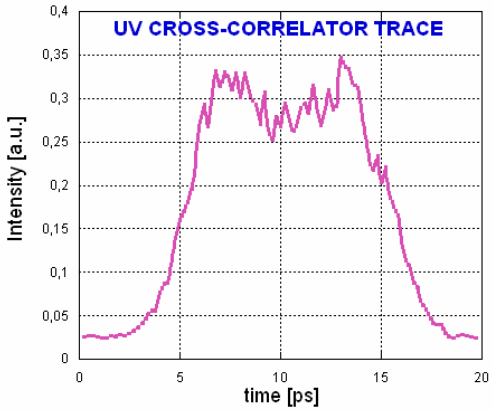

Figure 19: Cross-correlation of the UV flat-top obtained with the DAZZLER pulse shaper.

LCM-SLM PULSE SHAPER

We now discuss to operation principles of the pulse shaping system based on the LCM-SLM (liquid crystal mask – spatial light modulator).

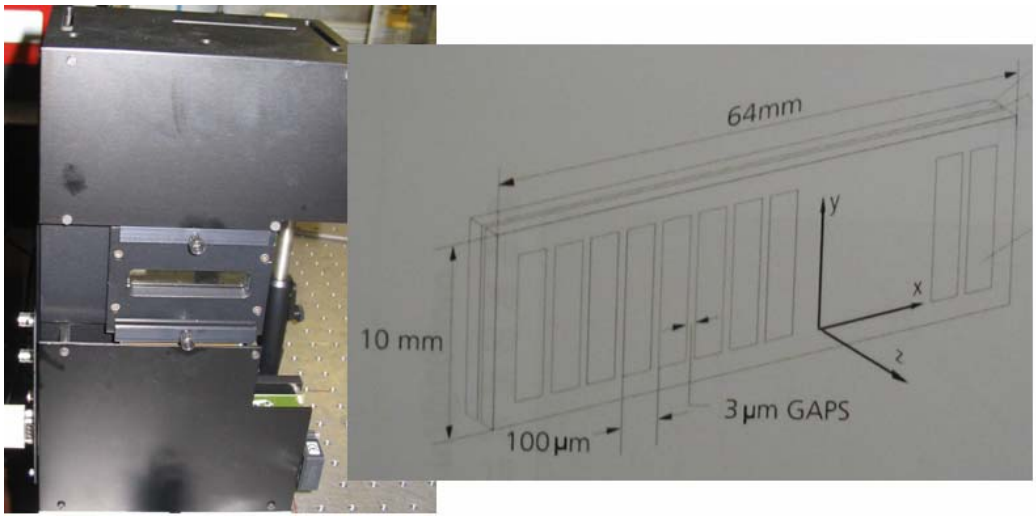

Figure 20: Picture of the Jenoptick SLM-S 640/12 and on the right the sketch of the liquid crystal array.

The mask is an array of pixels interleaved with small gaps (Figure 20). The mask chosen for the SPARC project is the Jenoptick model SLM-S 640/12. The dimensions of the pixels and gaps are, respectively, 97 and 3 μm wide, and the number of pixels is 640.
By changing the voltage applied to a single pixel it is possible to change the refraction index for that particular pixel. In this way, it is introduced a wanted phase shift in the radiation travelling trough the pixels. A LabView program has been developed in order to control the voltage applied to each pixel composing the liquid crystal mask.
The pulse shaping with the LCM-SLM is carried out introducing a proper spectral phase in order to obtain the wanted pulse intensity in the time domain.
In order to introduce the proper phase on the pulse it is necessary to propagate the different pulse wavelengths trough the individual pixels of the array. This is possible by using an optical layout called 4f which is reported in Figure 21. The set-up is composed by two anti-parallel identical gratings and two focusing lenses with focal length f. The optical elements are placed as reported in the figure. The wavelengths are dispersed by the first grating, and then the first lens collimates the laser frequencies. The second lens and the last diffractive optics are used to recombine the wavelengths with no residual spatial chirp and without temporal dispersion. The mask is located at the Fourier plane of the system where the spectral components of the pulse are linearly dispersed and focused. The 4f layout shown in Figure 22 has been designed to be compact in order to fit the space available on the optical table. The picture of the apparatus is shown in Figure 23. The overall energy losses are comparable with the DAZZLER ones.

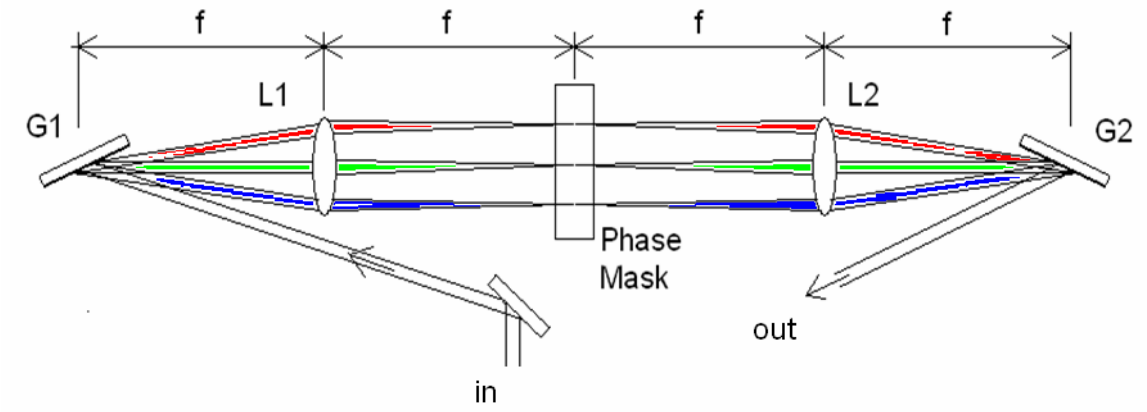

Figure 21: 4f optical setup. The diffraction grating G1 is used in order to apply a linear angular dispersion onto the input wavelengths. L1 is used to focus the spectral component at the Fourier plane where the mask is placed. The second lens and the output grating are positioned in a symmetric position and are used to recombine the wavelengths at the exit.

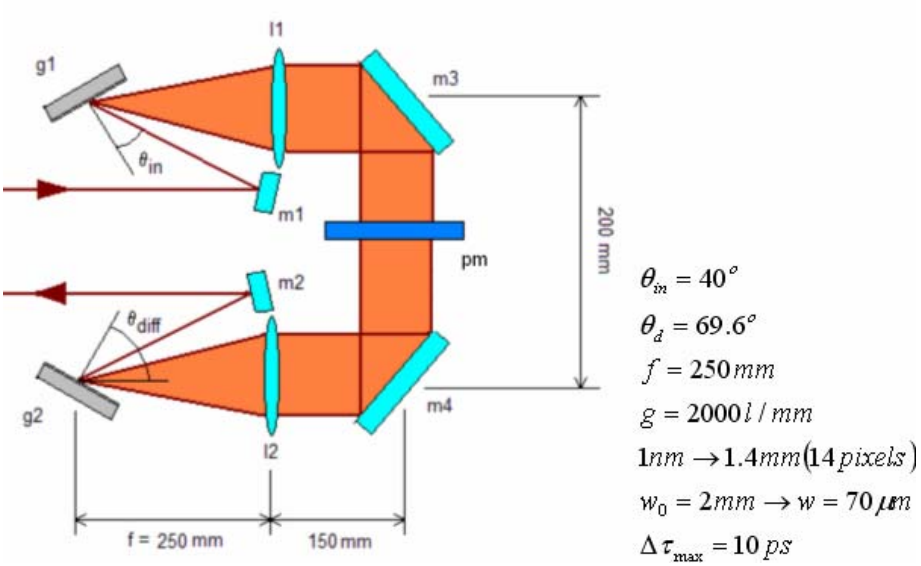

Figure 22: 4f optical setup implemented on the SPARC laser system

The phase function introduced by the mask and which is simulated is changed by modifying the coefficient of the following polynomial function

$$\phi(\omega) = \alpha \cdot (\omega - \omega_0) + \frac{1}{2}\beta \cdot (\omega - \omega_0)^2 + \frac{1}{3!}\gamma \cdot (\omega - \omega_0)^3 + \ldots$$

The first order coefficient "α" of the polynomial function brings a time shift of the pulse without changing its shape, the second order "β" induces a linear dispersion effect stretching or compressing the pulse and "γ" introduces a right or left asymmetry on the pulse shape. For our purposes the first four term of the polynomial function are sufficient.

The strategy that we studied and followed to obtain the results reported in this paper is based on the fact that, as said before, using the UV stretcher, the spectral profile can be converted into the time profile. We looked for a spectral phase modulation to introduce in the first harmonic pulse by the liquid crystal mask, capable to yield a third harmonic rectangular spectrum profile. The optimal phase function search was guided by the ORFEO simulations. In general a good strategy is to use the second order phase to enlarge the third harmonic bandwidth. At that point with the forth order phase we shrink the spectral tail and are able to

make a square-like spectrum in the UV. The third order is used to compensate possible pulse spectrum asymmetry.
For the liquid crystal mask, the phase function modulation can be quickly introduced and it is possible to see in real time the changes of the UV spectrum. This characteristic makes this device suitable to be integrated with an adaptive algorithm.

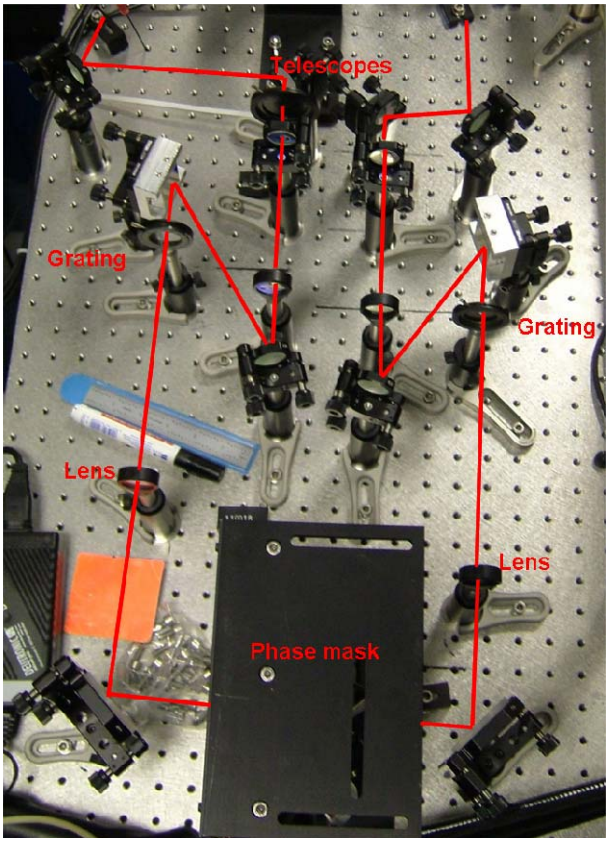

Figure 23: Picture of the 4f optical setup where is evidenced the optical path.

A critical point of LCM-SLM is the alignment of the system. In fact, it is not easy to perfectly align the 4f configuration in order remove any undesired effects such as spatial chirp and beam divergence of the output beam. This consideration is true especially when the optical setup is realized in small room, as in our implementation. The residual spatial chirp out of the 4f system is particularly deleterious since it seeds the regenerative laser. This amplifier is characterized by its own cavity's spatial and longitudinal modes. So, to avoid undesirable amplitude modulation of the amplified IR pulses, it is absolutely necessary that all the spectral components of the pulse coming out the 4f be well matched with the spatial modes of the RGA cavity. It is then clear that a diagnostic device for the IR before and after the RGA is mandatory to correctly align the 4f apparatus.
According to our experiences, when the chirp has been minimized out of the 4f setup it is important to accurately stir the regenerative input beam in order to produce an undistorted output spectrum out of the amplifier cavity. Anyway the output spectrum is very sensitive to even small misalignment of the seed beam and requires a real time control.
Once the alignment is done, the spectral amplitude is not influenced by the phase modulation and with the mask it is possible to control the IR manipulation up to the exit of the amplifier.
Using the simulation code to take into account the alteration introduced by the third harmonic generation it was possible to achieve the flat top with 2.1 ps rise time. In Figure 24 it is reported the cross-correlation trace of the UV pulse. The ripples on the plateau are enhanced by shot-to-shot amplitude fluctuations recorded during the measurement.

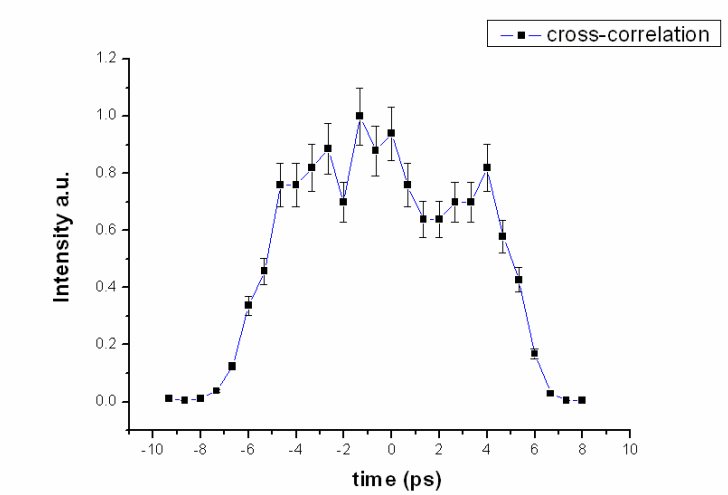

Figure 24:Cross-correlation of the UV flat top pulse obtained with the LCM-SLM shaper.

We have also theoretically and experimentally verified that in order to manipulate the UV spectral profile by the phase function introduced in the fundamental, the bandwidth of the IR beam must not be too large (~10nm) otherwise the third harmonic spectrum starts to be excessively modulated by the BBO crystal bandwidth and it becomes difficult to introduce the desired phase modulations and reduce the rise time. To prevent this undesired effect in the Fourier plane we added two metal sheets to block the tails of the spectrum.

DISCUSSION

The shaping system based on the SLM is more complicated to be aligned with respect to the system based on the DAZZLER. For this reason the scheme 4f + SLM, from a maintenance point of view, is more critical also for the fact that the IR spectrum before and after the regen amplifier must be checked continuously.
The SLM requires to be found the calibration constant that allows converting the voltage applied to the single mask's pixel and the actual phase shift, between 0 and 2π, added to the optical wavelength.
Nevertheless the advantage of this scheme compared to the DAZZLER one is the better resolution and that the phase modulation can be introduced more quickly, therefore an iterative system can be simply implemented in order to find out the best modulation function.
This is basically what has happened in our case: using the DAZZLER we were not capable to obtain rise and fall time shorter that ~2.6 ps while with the SLM we obtained ~2.1ps for the same parameter values. We believed that this can be attributed to the smaller number of optimization attempts we did when the DAZZLER layout was used.
Anyway in both cases the rise and fall time is larger than 2 ps and we could not obtain faster edges. The reason for this is the smoothing effect on the UV spectrum due to the third harmonic generation process.
We have been capable to overcome this problem obtaining ~1.4 ps for the same parameter values by changing the shaping device system. Summarizing, in the new shaping scheme, we sent the IR Gaussian spectrum into the amplifier without introducing any modulation in the IR. Then we used a modification of the UV stretcher to perform a cut of the UV pulse spectral tails. By controlling the cut sharpness it is possible to generate overshoot in the time profile that compensates the curvature that would correspond to a truncated Gaussian spectrum. This new scheme let us to simplify the all procedure to manipulate the pulses obtaining not only the target shape but also more exotic profiles as for example the multi-peaks.

INFN - MI

1) The R&D on UV rectangular laser pulse generation has been performed according to the proposal. Tests of an optical apparatus based on a new principle have been done. In the scheme, which we believe is novel, the longitudinal profile of a laser pulse from a Ti:Sapphire master oscillator power amplifier system is controlled using a mechanical mask in the Fourier plane of a 4f stretcher located after the harmonic conversion crystal. Such a scheme allows us to overcome many of the difficulties faced by current state-of-art pulse-shaping designs. Beyond the clear advantages of simplicity and robustness, the proposed solution offers the possibility to deliver a pulse with very short rise and fall times and to freely change the output length. The USA company RadiaBeam has contacted the authors of the new optical apparatus for a possible production.

2) We have continued the investigation of the generation of sub-picosecond multiple electron trains generation in a RF electron gun by corresponding patterned laser trains for electron pulse trains useful for Far Infrared Radiation generation. The case of twin-pulse high quality electron beams were been especially treated for optical light FEL twin -pulse generation interesting for pulse-pulse experiments.

3) We have also performed a systematic analysis for the generation of single shaped electron bunches in the RF electron gun of the SPARC accelerator aiming to obtain single-spike FEL operation.

4) We have made some tests on the Phase-Coding system of the CTF3-CERN project. In particular we have checked the losses of the optical component of the system, finding that the fiber launch, the modulator, the fiber beam splitter and the fiber-fiber junctions have losses about a factor two above those claimed by companies. We have then made successfully the test of the principle of operation of the entire Phase-Coding system. as shown in Figure 25.

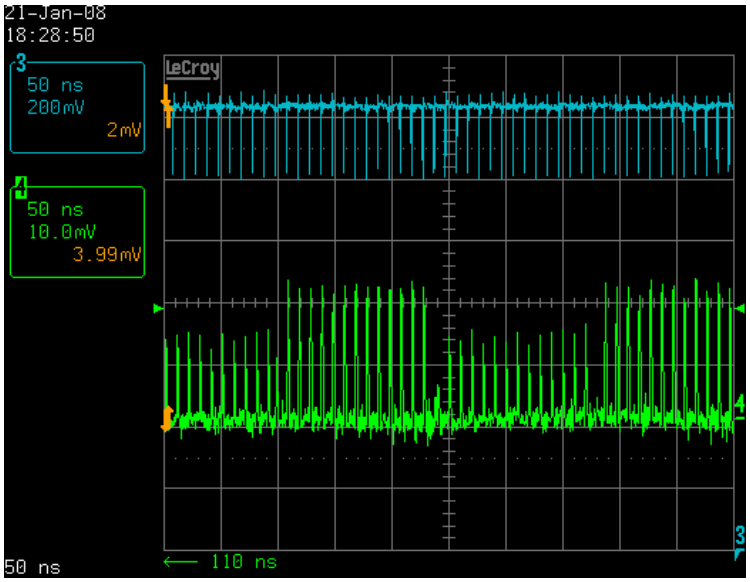

Figure 25: Sub-trains of right lengths are generated.

WP 4, RF GUN AND BEAM DYNAMICS

CERN

The installation of the PHIN photoinjector in CTF2 building for off-line commissioning has been completed (see Figure 26). It remains to install the RF wave guides at 3 GHz.

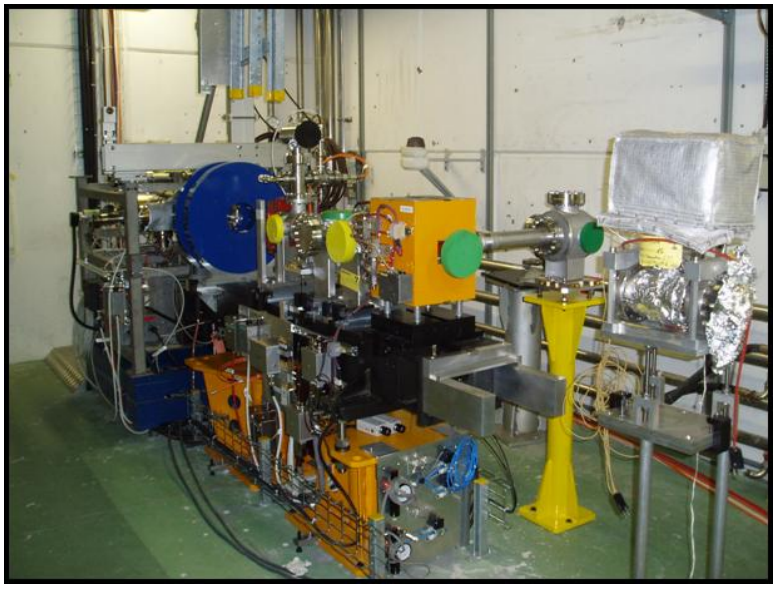

Figure 26: PHIN photo-injector line installed into the CTF2 building at CERN

LAL

The definitive model of the gun was matched according to the specifications the 18th of December 2006. But after a re-machining of the cells (to clean it), a black spot appeared on the surface of one cell. It was decided to send it to CERN for analyses.

For some time CERN put its veto on brazing since from the analysis of the surface of the RF cell, CERN metallurgists suspected that the copper used was not forged. The surface seemed to present in fact micro-porosity, which could lead to virtual leaks in operation, and also several inclusions. Therefore this cell was thrown away and replaced by its twin which was part of the second identical RF gun aimed to be installed in the NEPAL station.

All pieces were sent to CERN the 8th of February 2007. The brazing of the tapered waveguides was done the 20th of April 2007 and LAL received it one month later. Then the waveguides have been machined to adapt LIL (LEP Injector Linac) flanges and sent to CERN in June. So the complete RF gun should have been brazed and available at LAL in September. But due to LHC constraints, the CERN brazing workshop was very busy; hence the brazing of the PHIN gun was delayed until the end of the year (see Figure 27).

In January 2008 vacuum tests have been performed and big leaks were found in the cooling circuit. The CERN brazing workshop will try to fix the problem. If it is successful the gun will then return to LAL for final measurements, tuning and welding of the NEG pumping chamber. LAL foresees to deliver the RF Gun for PHIN in April 2008.

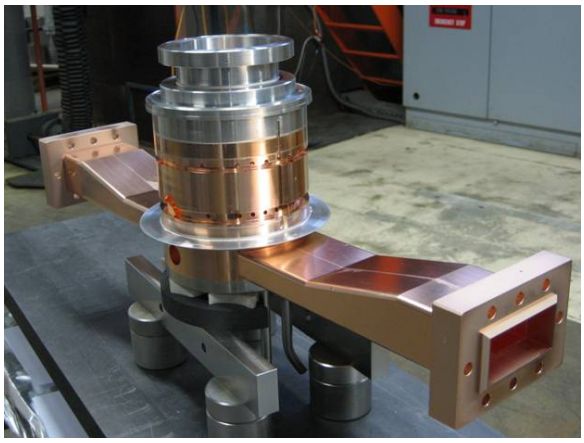

Figure 27: PHIN RF gun after brazing

NEPAL STATION

In 2007, civil engineering required for the upgrade of the shielding has been finished in October. Yet, we have been prevented to install because of legal obligation to first remove asbestos. Most of the heavy and bulky elements as the bench supports will be installed as soon as the Nepal room entrance reconstruction will be achieved (foreseen during the first week of February 2008).In spite of this difficulty, the main electric switch board is ready. After a first examination of our preliminary radiation safety document by the French Nuclear Authority Agency (ASN) in October 2007, we have transmitted to them the full corrected document in January 2008.

A drawing of the accelerator is shown in Figure 28. Lot of components are already available: girder, modulator, klystron, solenoids with its power supply, steerer and dipole. The RF network is designed and foreseen to be provided by the tender in June 2008. The RF gun which is a copy of the one done for CERN and should have been brazed at CERN is finally brazed at LAL. It should be finished in mid-March.

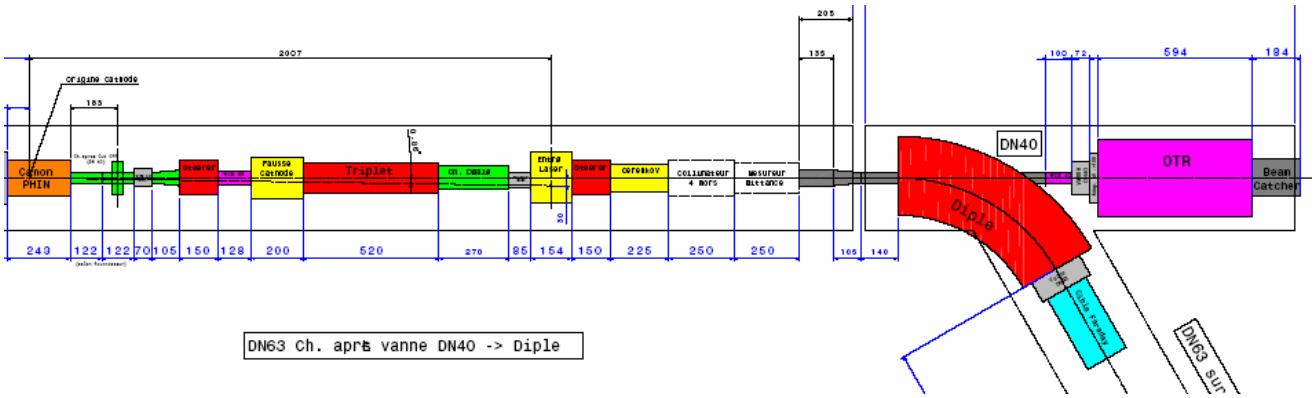

Figure 28: Layout of the NEPAL beam line.

Because of a lack of funds some components are delayed as a booster to rise the beam energy up to 10 MeV and the device for emittance measurements.

Simulations of the beam dynamics of this new version of the accelerator have been performed with PARMELA. Results are shown in Figure 29. With charge below 2 nC, beam can be transported without losses in the deviated beam line.

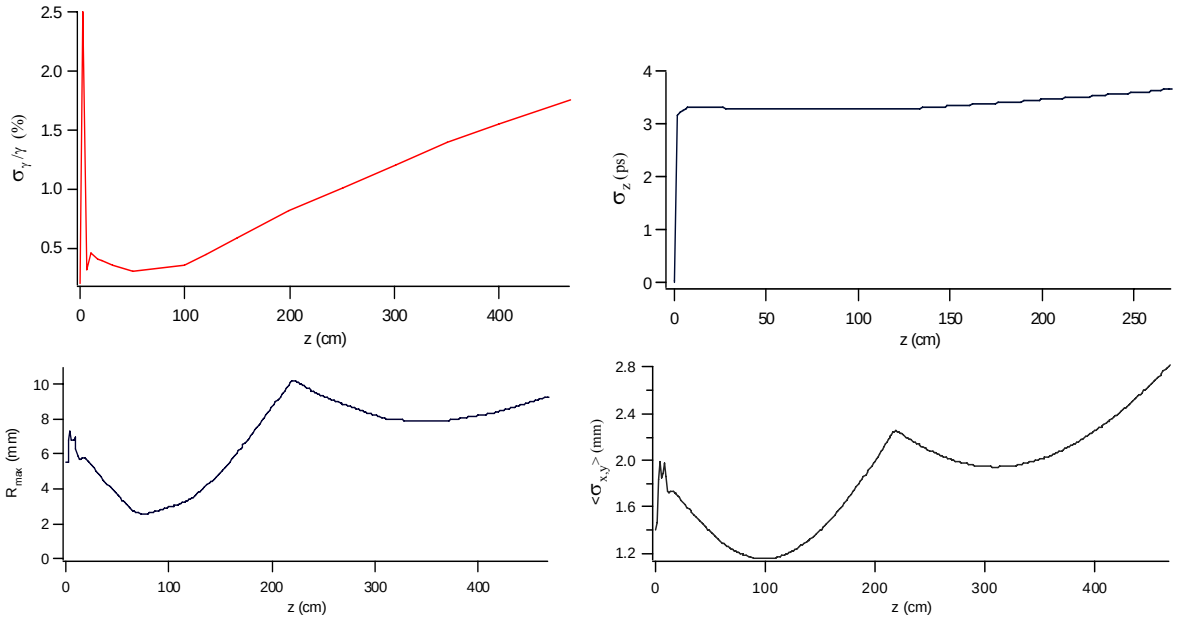

Figure 29: results of beam dynamics simulations with the PHIN gun, solenoids on the gun and another one at z = 210 cm, Q = 1 nC. Left up corner, rms energy spread; right up corner, rms bunch length; left bottom, maximum radius of the beam; right bottom, rms size of the beam.

LOA

A single shot compact electron spectrometer has been developed in order to measure the electron spectrum that will be produced in future laser plasma accelerator experiments. Electron beams produced in such accelerators have an energy distribution which is composed by a thermal distribution at low energy and by a quasi mono-energetic peak at high energy. For this purpose, this broadband spectrometer has been design in order to give access to the full electron energy distribution. It has been also tested at LOA. The B field distribution values have been found to be in very good agreements with the calculated one. The corresponding detailed report is on the CARE website as CARE report 07-034.

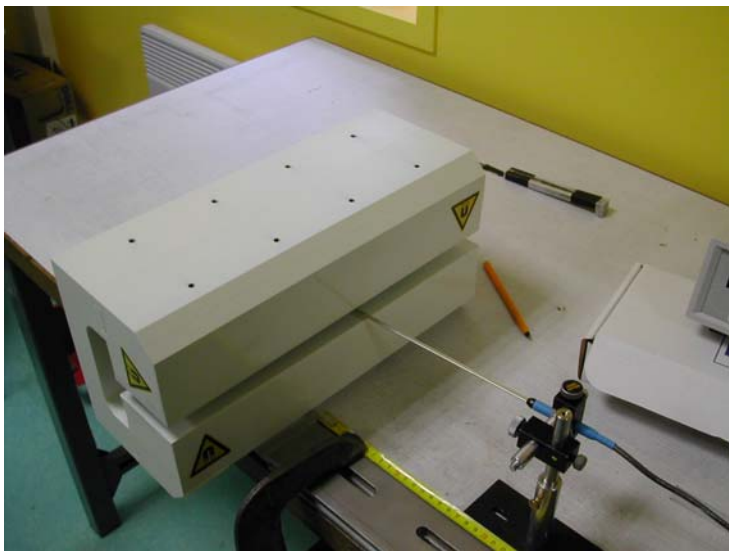

Figure 30: Experimental set up for the measurement of the magnetic field

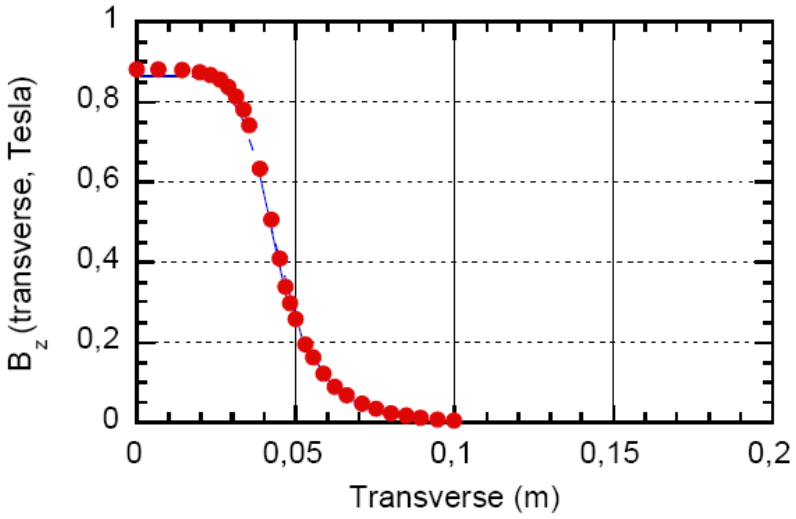

Figure 31: Experimental results (red dots) and simulation (blue line)

FZR

After the final test of the niobium cavity in the vertical test bench and the He tank welding, the assembly of the cryostat started in spring 2007. During the summer shutdown of ELBE in June and July 2007, the cryostat and the first part of the beam line were installed in the accelerator hall as it is shown in Figure 32. The cryostat was connected to the He supply line of the ELBE refrigerator and the first cool-down was performed at the beginning of August 2007. In the following weeks the RF system was put into operation. Tests and measurements with low-power and later with high-power RF were carried out. At the same time the 500 kHz UV laser system was delivered and tested by MBI, and the optical components of the laser beam line were installed and adjusted.

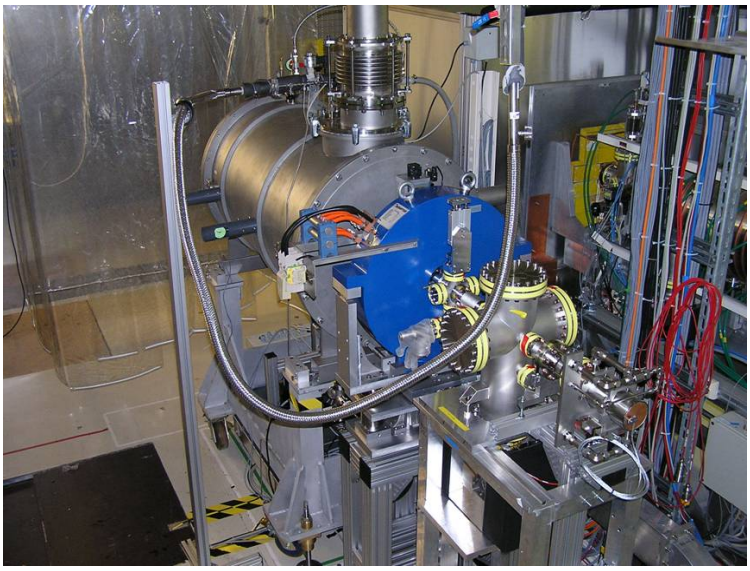

Figure 32: The SRF gun installed in the accelerator hall
with emittance compensation solenoid and laser input port.

The autumn shut-down of ELBE, in October 2007, was used to complete the installation of the diagnostics beam line. Designed and constructed by BESSY, this beam line is needed for the test, characterization and optimization of the SRF gun. Beside an emittance compensation solenoid downstream the gun and the beam optical components like quadrupoles and steerers, the beamline contains a diversity of diagnostics units as shown in Figure 33. A Faraday cup, integrated current transformers (ICT) and beam dumps allow beam current measurements. Energy and energy spread can be determined by means of a C bend magnet. The transverse emittance of the beam can be measured with a slit mask system (EMS) and for the determination of bunch length two methods will be applied: Cherenkov radiation measurement with the streak camera and electro-optical sampling.

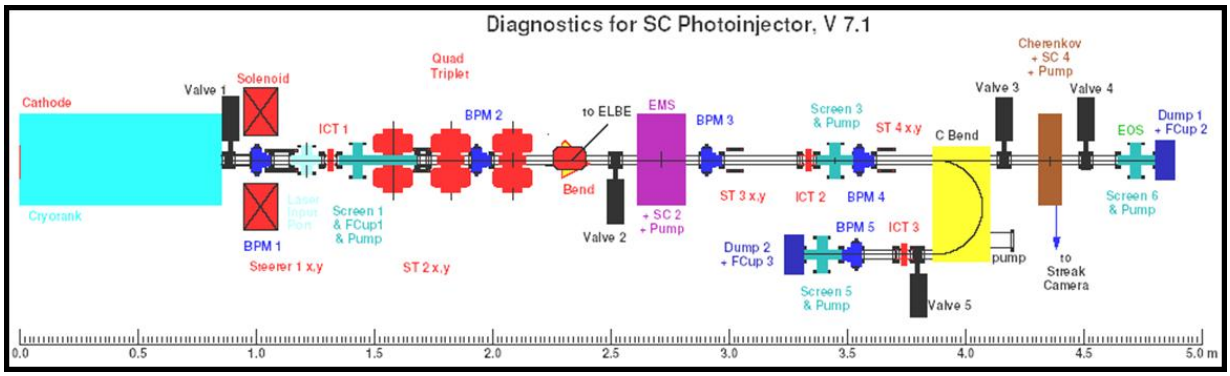

Figure 33: Diagnostics beamline installed at the SRF gun.

End of October, the gun was cooled down for the second time. After readjustment of the laser beamline, putting into operation the power RF, the vacuum system, screen stations and some other components of the diagnostics beamline, the first electron beam could be produced on November 12, 2007. Until end of 2007 the beam time was used for commissioning and test of further diagnostic components in the beam line and for a first characterization of the electron beam. The following measurements concerning the cryogenic, RF and beam properties of the SRF gun have been performed or started in 2007:

1. Static heat losses of the cryostat,
2. He pressure stability, He level control and interferences with the other cryostats,
3. Cool-down curve and temperatures in the cryostat, operation at 2 K,
4. Cavity frequency during cool down,
5. Pass band frequency and field distribution at 2 K,
6. Phase and amplitude stability of the low level RF system, microphonics,
7. Cavity performance (quality factor versus gradient)
8. He pressure sensitivity on the cavity tuning,
9. Lorentz force detuning,
10. UV laser power and spot size at the photo cathode (virtual cathode),
11. Photo current and quantum efficiency of the Cu photo cathode
12. Electron beam spot size,
13. Electron current and bunch charge,
14. Electron energy,
15. Laser phase scan (transmission and energy).

As an example Figure 34 shows cavity performance curve (quality factor versus acceleration gradient) of the 3½-cell cavity in the gun operated at 2 K. As earlier observed in the vertical tests, the gradient is limited by field emission starting at an acceleration gradient of about 5 MV/m which belongs to an peak field value of 14 MV/m in the cavity cells. The electron

beam was generated from a Cu photo cathode with a laser power of about 0.4 W at a repetition rate of 100 kHz and an acceleration gradient of 5 MV/m in the gun cavity. The beam could be imaged onto the YAG screens in the diagnostics beamline. In this case the bunch charge was about 0.5 pC. Fig. 35a shows a typical picture with beam on screen 1 and the solenoid switched off. On Fig. 35b the beam is focused on screen 1 with the emittance compensation solenoid (31.5 A).

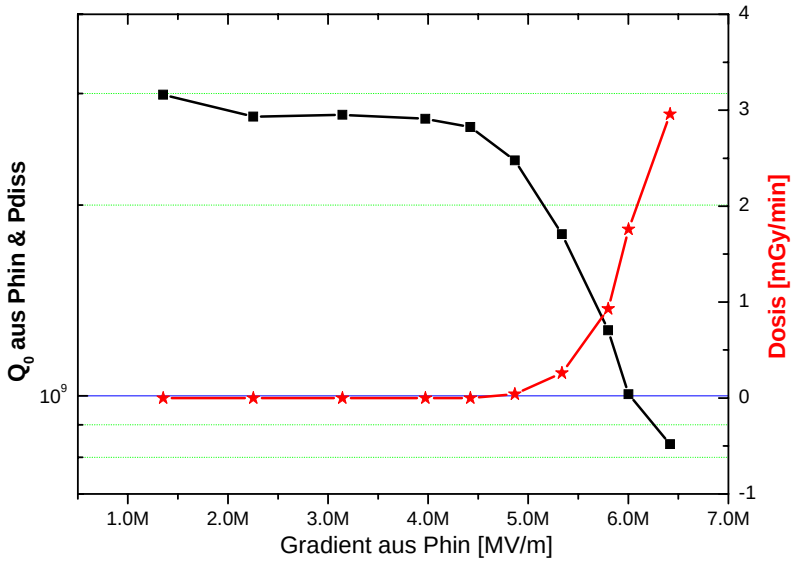

Figure 34: Quality factor Q_0 versus acceleration gradient and corresponding field emission dose.

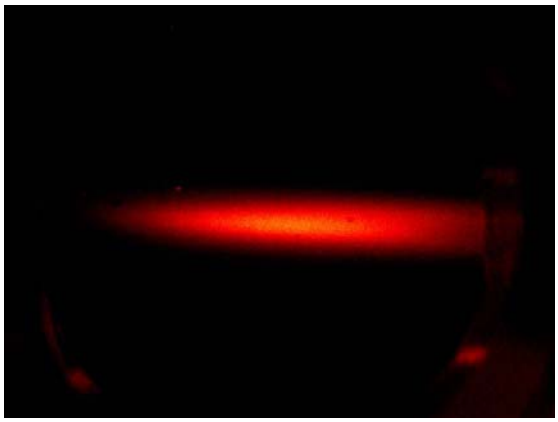

Fig. 35a: Electron beam image on screen 1, solenoid switched off.

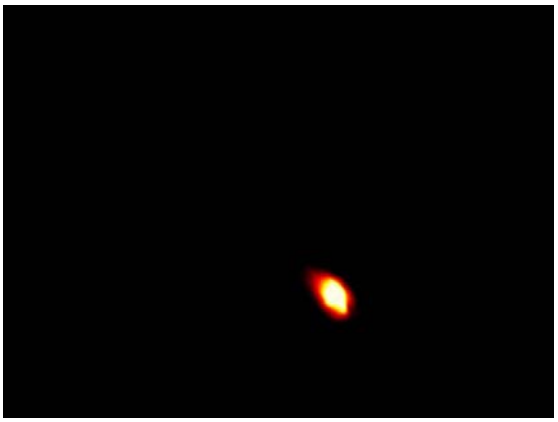

Fig. 35b: Electron beam image on screen 1, focused with the solenoid (I = 31.5 A), spot size 1.0 mm x 1.2 mm FWHM.